RF emission spectra in laser-plasma acceleration of protons

M. Seimetz[1]
1. Instituto de Instrumentación para Imagen Molecular (I3M), CSIC-Universitat Politècnica de València, Valencia, Spain

Contact: mseimetz@i3m.upv.es

Abstract
The acceleration of protons and ions by highly intense, ultra-short laser pulses is a very active field of experimental and theoretical research. The emission of a strong electromagnetic pulse (EMP) has often been reported as a side effect of laser-plasma interactions. It potentially interferes with, or even may cause damage to, electronic devices such as particle detectors inside or outside the vacuum system. A better understanding of the sources of rf emission may be highly relevant for several practical aspects including efficient EMP suppression.
We have used the RF module of COMSOL® Multiphysics to model the essential components of a complete experimental setup for laser-proton acceleration and to identify the major sources of EMP. The basic example of a cylindrical cavity representing the principal vacuum vessel allows for reproducing the fundamental modes (which can be readily compared to analytical solutions) as well as higher modes. Several parts of the vacuum system have then been added to the setup to study the appearance of corresponding eigenfrequencies.
In addition to the cavities, internal components act as microwave antennas. Those elements which are most likely to transfer electric currents due to the emission or absorption of charged particles, such as the target holder, have been implemented in the simulated compound. Even with simplified geometries their resonant frequencies contribute significantly to the overall rf spectra. Further, modulations of the cavity spectra due to interference with the internal parts have been observed as well.
At high frequencies (in our case, at 1.0-2.5 GHz) the density of simulated modes increases strongly, making it necessary to evaluate quantitatively the contribution of single modes to the overall EMP amplitudes. COMSOL® offers two distinct definitions of quality factors corresponding to each eigenfrequency. Their adequacy as weighting factor for a complete spectral representation has been studied.
The simulated EMP spectra compare reasonably well to experimental data. Our results will be applied as an analysis tool for laser-plasma interactions from different targets.

Keywords: EMP, rf eigenmodes, cavity, laser-plasma interaction

Introduction
Plasma formation by ultra-short, ultra-intense laser pulses interacting with solid targets has become a very active field of research covering a range of phenomena such as laser-ion acceleration, inertial confinement fusion, and laser ablation[1]. One of the phenomena associated to laser-plasma interaction is the emission of an electromagnetic pulse (EMP). While initially reported as an unwanted side effect, the origin of radiofrequency (rf) radiation in related experiments has recently attracted considerable interest as a potential tool for the analysis of the underlying physical processes. In fact, at least three distinct sources of EMP have been identified: strong currents in the plasma plume[2,3], neutralisation currents inside the target holder[4], and oscillations of the vacuum systems excited by the impact of charged particles[5,6]. These may involve different time scales, and hence, leave fingerprints in the rf spectra starting from a few MHz to tens of GHz or beyond.
The present work aims at identifying the major sources of electromagnetic noise in a laser-proton acceleration experiment realised with a 3 TW, 55 fs Ti:Sapphire laser[7]. Its pulses are focalised on thin foil targets with intensities exceeding 10^{18} W/cm^2 and giving rise to large numbers of protons with energies up to 2 MeV.

The target holder as well as optical components and particle detectors are mounted inside a system of vacuum chambers and tubes. As was first recognised by Mead *et al.*[5] the target chamber of a laser-plasma experiment, when struck by intense bunches of charged particles, effectively acts as microwave cavity. Its fundamental resonance modes can be calculated analytically as long as the geometry is close to a cylinder or brick. More recently simulations with COMSOL Multiphysics® have revealed how details of the setup (in this case, at the PALS facility) have influence on rf emission[8]. Inspired by this reference we have applied COMSOL Multiphysics 5.3a to study the resonance frequencies of our vacuum system. Starting from a very basic, cylindrical chamber, an increasing number of components has been implemented in order to understand the corresponding rf spectra. Details of these simulations are presented in this paper. A comparison to experimental data is left for a separate publication.

Theory

Oscillating electric charges in conductive cavities can form standing waves corresponding to eigenfrequencies. These can be calculated analytically in the case of basic geometries with translational or angular symmetries[9,10]. Our target chamber, as well as other components of our setup, can be approximated by cylinders of height, l, and radius, a. Then the lowest resonant frequency, f_0 (denominated TM_{010} mode), is[9]

$$f_0 = \frac{2.405\ c}{2\pi a} \quad (1)$$

with c, light speed (here, in vacuum). The next higher modes have frequencies

$$f_0 = \frac{c}{2l}\sqrt{1 + \left(\frac{2l}{ka}\right)^2} \quad (2)$$

where k = 3.41 (TE_{111}), 2.61 (TM_{011}), and 1.64 (TE_{011}), respectively.

An important parameter of a resonant cavity is its quality (or Q-)factor which is computed as

$$Q_1 = \pi\frac{f_0}{\gamma} \quad (3)$$

with the damping factor, γ which governs the time evolution of the field amplitude. The Q-factor also relates the energy stored inside the cavity volume, W_t, with the power dissipated from its walls, P_d, via

$$Q_2 = 2\pi f_0 \frac{W_t}{P_d}. \quad (4)$$

For ideal cavities both definitions coincide numerically.

Simulation of rf cavities

Our study has been carried out with the RF Module of COMSOL Multiphysics 5.3a. It is based on a tutorial example calculating the resonant frequencies and Q-factors of cavities with lossy walls[11]. In fact, the range from 0.1 to 2.5 GHz and the typical dimensions of our structures (0.1-0.6 m diameter) justify working in the frequency domain. Maxwell's equations take the form

$$\nabla \times (\mu_r^{-1}\nabla \times \boldsymbol{E}) - \frac{\omega^2}{c^2}\left(\varepsilon_r - \frac{i\sigma}{\omega\varepsilon_0}\right)\boldsymbol{E} = 0 \quad (5)$$

with $\omega = 2\pi f_0$, the relative permeability, μ_r, the relative permittivity, ε_r, and the electrical conductivity, σ. Impedance boundary conditions apply with vanishing surface current,

$$\sqrt{\frac{\mu_0\mu_r}{\varepsilon_0}}\boldsymbol{n} \times \boldsymbol{H} + \boldsymbol{E} - (\boldsymbol{n}\cdot\boldsymbol{E})\boldsymbol{n} = 0\,. \quad (6)$$

As a first step the simulated geometry is limited to a cylindrical, metallic chamber of 0.6 m diameter and 0.3 m height, corresponding to the vacuum vessel containing the laser target and focussing optics. COMSOL straightforwardly identifies a series of eigenmodes. The electric field geometry of the fundamental (TM_{010}) mode (Figure 1) corresponds to examples from text books[9,10] and its eigenfrequency (382 MHz) matches with eq. (1).

The next higher simulated modes are identified as TE_{111} (579 MHz), TM_{110} (609 MHz), TM_{011} (629 MHz), TE_{211} (697 MHz), TM_{111} (788 MHz), and TE_{011} (788 MHz) (the two TM_{111} and TE_{011} are degenerate). Three of them match very well with those of eq. (2). Associated to each eigenfrequency COMSOL computes the Q-factors of eqs. (3) and (4). For the basic

geometry of Figure 1 the numerical results for Q_1 and Q_2 are very similar to each other.

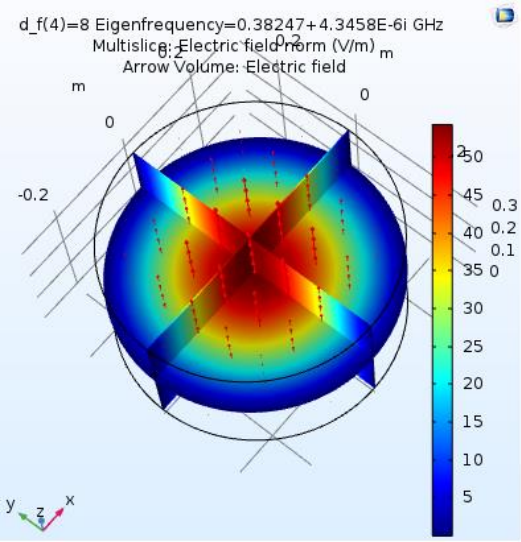

Figure 1 Fundamental mode of the target chamber.

A major modification to the "perfect" cavity is introduced by replacing the top end cover of the cylinder by a glass plate (corresponding to our experimental setup). This disturbs the symmetry of some of the standing wave patterns. In addition, the TM_{010}, TM_{110}, TM_{011}, and TM_{111} modes are significantly shifted towards higher frequencies (by 5-21 MHz) while TE_{111}, TE_{211}, and TE_{011} undergo much smaller, negative variations (3-4 MHz). TM_{111} and TE_{011} are no longer degenerate. Another striking observation is that the two Q-factors given by COMSOL now are completely different to each other. While Q_2 is of similar magnitude as before Q_1 becomes smaller by about four orders of magnitude. This indicates a strong damping of the modes related to the target chamber.

At this point it is helpful to propose a graphical representation of the eigenfrequencies. As in our experiment spectra up to 2.5 GHz will be extracted we aim at identifying all the eigenmodes up to this limit. In COMSOL this is done by searching for series of eigenfrequencies (e.g., 24 at each time), but with different start values. When plottet in a histogram (Figure 2) close-by or degenerate modes appear as multiple counts in a single bin.

A system of vacuum tubes is then added to the simulated geometry. It comprises a 2 m long tube for time-of-flight measurements, a similar one connected at an angle of 90°, and a second vacuum chamber of the same size as the target chamber. All components are made of metal

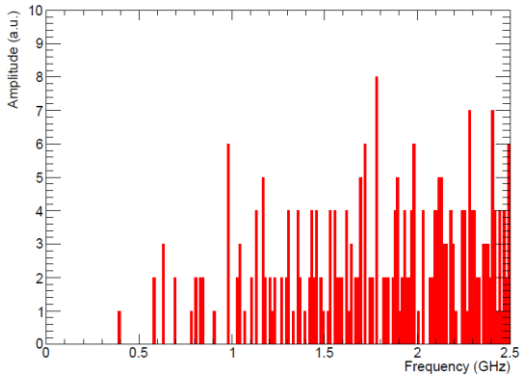

Figure 2 Eigenfrequencies of the target chamber.

(actually, the predefined "lossy wall" material of COMSOL) except the top cover of the vessel which is of glass. Here again, we search for all eigenmodes up to 2.5 GHz. An important observation is that the components tend to ring individually, above all in the low-frequency regime. As the large vessels are identical the modes obtained from the target chamber alone now appear twice. The first resonances of the vacuum tubes are observed just above 1 GHz. For example, the TE_{111} mode of the time-of-flight tube (Figure 3) is found at 1.17 GHz, in agreement with eq. (2). Since here the ratio $l/a >$ 2.03 this is the fundamental mode, not TM_{010} as above[10]. Starting from 1.18 GHz we also find coupled eigenmodes of two or more components. In this way the number of frequencies increases tremendously. However, only very few emission lines appear below 1 GHz.

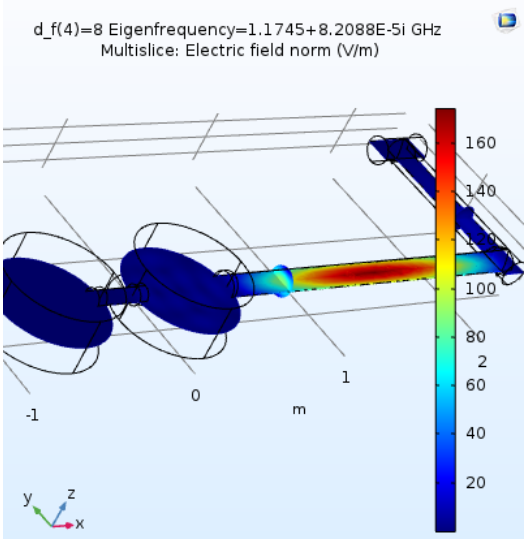

Figure 3 TE_{111} resonance of the flight tube.

Rf emission by internal components

Radiofrequency waves can also be emitted from metallic objects inside our vacuum system acting as antennas. As a simple test we consider a thin rod of 0.5 m length floating freely inside our target chamber. Both are made of the same "lossy wall" material (a control test with steel has not led to significantly different results). In COMSOL, after carefully defining its geometry as well as the difference of the surrounding and interior volumes[12] (see inset of Figure 4), the eigenfrequency search proceeds as before. What we find is an emission at 248 MHz which does not quite correspond to the 300 MHz expected from a λ/2 antenna. It is followed by the fundamental mode of the chamber at 382 MHz. If the length of the rod is modified the emitted frequency changes accordingly.

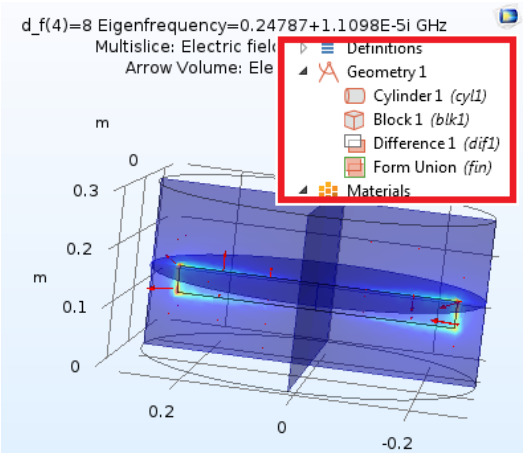

Figure 4 Free metallic rod inside the target chamber.

This now enables us to define more complex geometries of objects related to our experiments. The target holder (Figure 5) is of special importance as it is likely to be subject to charged currents after the laser-plasma interaction. It consists of a metal frame held by two perpendicular step motors for precise positioning. We have chosen a rather coarse representation in COMSOL. The entire structure is connected to the bottom cover of the vessel and the space intended for carrying thin target foils is left empty. This object strongly alterates the rf spectra as compared to an empty vessel (here again, with a top cover made of glass). First, an "antenna mode" appears at 239 MHz which corresponds to a rod of the total length of the bent holder structure (arrow in Figure 6). Second, the fundamental frequency is moved to 416 MHz. And third, the rotational symmetry of the chamber is destroyed and modes with two (x, y) orientations are no longer degenerate, resulting in additional lines at higher frequencies.

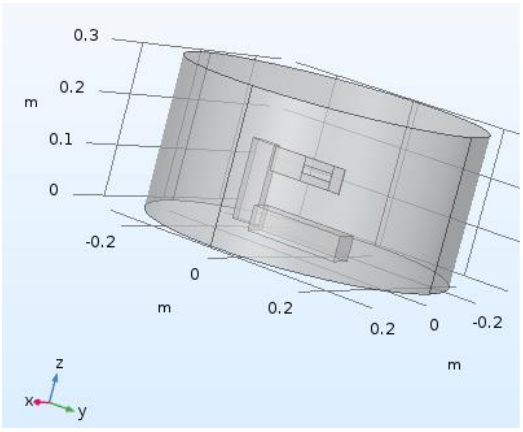

Figure 5 Model of target holder inside the chamber.

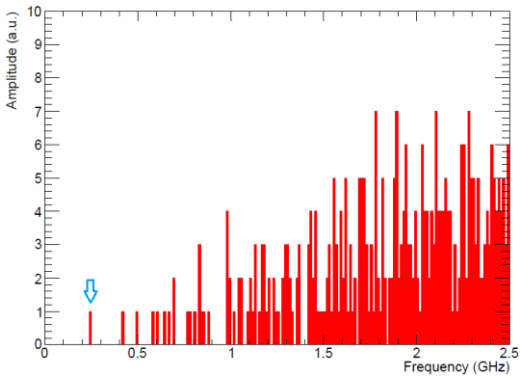

Figure 6 Eigenfrequencies of chamber with target holder. The arrow indicates the "antenna" mode.

One may argue that the representation of the target holder is over-simplified. Its real-world fine structure may introduce a wealth of resonant modes rather than the single line of Figure 6. To corroborate this we have inserted the complete geometry of a stepper motor inside our vacuum vessel using the COMSOL CAD Import module. It comprises tiny parts which require a much finer mesh than before. Correspondingly, the computation time increases by two orders of magnitude. The result, however, is basically the same as before. The typical size of the details of the motor structure is much smaller than the rf wavelength and therefore they do not alterate our frequency spectra.

At this point we have also checked the influence of lateral, dead ports of the vacuum chamber but we found only minor shifts in the spectral part

below 0.9 GHz. We thus conclude that internal components are more likely to account for rf lines in the low-frequency regime.

Complete geometry

In an attempt to simulate all relevant components together we have introduced the target holder and two additional support structures in the "complete" geometry of Figure 7.

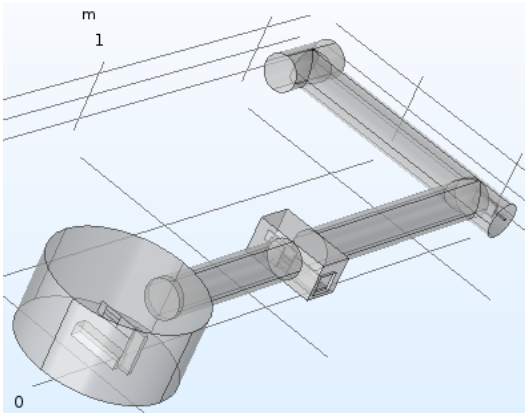

Figure 7 Complete geometry with vacuum tubes and internal components.

COMSOL identifies about 550 eigenfrequencies of this setup in the range from 0 to 2.5 GHz. Some belong to single components, others are oscillating modes of two or more parts. Figure 8 shows all lines classified according to the resonant parts. The "antennas" (internal components) ring at low frequencies; only one eigenmode is found for each of them.

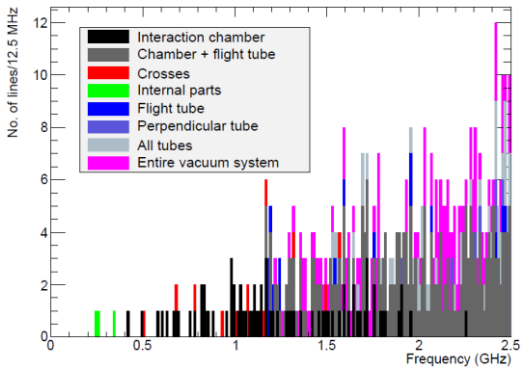

Figure 8 Eigenfrequencies of the complete geometry, separated by components.

The big interaction chamber dominates the spectrum up to 1.2 GHz and numerous common modes of this vessel and the flight tube are identified above 1.7 GHz. The vacuum tubes come into play at 1.2 GHz approximately with many modes at higher frequencies. And resonances with electric fields in all vacuum parts become especially important above 2 GHz. The question is now which of these modes actually contribute to EMP, and what are their relative amplitudes. As mentioned above, COMSOL offers two Q-factors which have very different magnitudes. The popular definition of eq. (4), Q_2, based on the stored energy and dissipated power, is especially high for the modes related to the interaction chamber (Figure 9). Q_1, to the contrary, takes damping into account which is produced mainly by the glass cover of the big vessel. As a consequence, the lines related to the chamber almost vanish (Figure 10) and the frequency spectrum is dominated by the vacuum tubes.

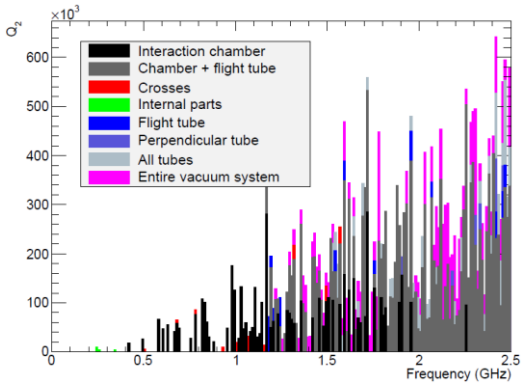

Figure 9 Eigenfrequencies of the complete geometry, weighted by Q_2.

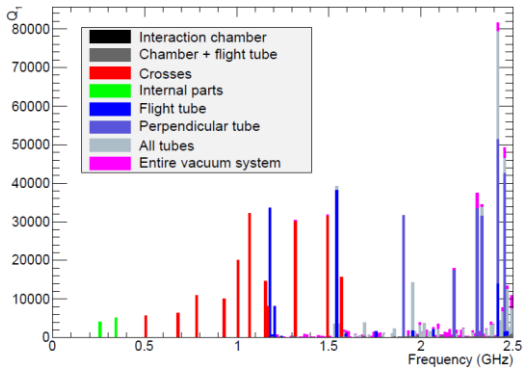

Figure 10 Eigenfrequencies of the complete geometry, weighted by Q_1.

Discussion

Several important conclusions can be drawn from our COMSOL simulations. In the low-frequency regime (up to 1 GHz) the number of eigenmodes is quite limited; most of them correspond to the laser interaction chamber. The target holder inside this vessel significantly alterates the spectra, especially because the symmetry is destroyed and some lines become

highly non-degenerate as compared to an empty chamber. Other geometric details such as dead ports do not introduce major changes and can therefore be omitted. In this context it has to be underlined that none of our tests has revealed eigenfrequencies below the fundamental mode of an empty vessel (382 MHz) with the exception of the internal parts. Similar observations have been made in two recent publications[13,14]. This may have important implications for the interpretation of experimental data whenever rf emission is actually observed at low frequencies. Other, possible sources should then be identified.

The components of the complete vacuum system show individual eigenfrequencies which correspond very well to theoretical expectations. This gives considerable robustness to the model; it seems reasonably safe to identify prominent peaks extracted from experimental data with single, simulated lines. Nevertheless, common resonances become increasingly important at high frequencies (above 1.5 GHz).

Above 1 GHz at least one simulated eigenmode lies close to *any* peak which may be found in an experiment. Therefore reliable criteria for the actual amplitude should be at hand. A large Q-factor alone is not meaningful in this context because it characterises the eigenmode but not its excitation. In a laser-acceleration experiment some components will be subject to the impact of electric charges and therefore ring strongly while others are not. It may also be reasonable to assume that transverse electric (TE) and magnetic (TM) modes will not be equally excited and that higher-order modes of the same kind will have smaller amplitudes than the fundamental ones. Building a complete model of rf emission in laser-ion acceleration would therefore require the implementation of charged particle deposition on the resonant structures, probably in a time-dependent way, and taking into account the excitation of each single mode. In that sense, the present simulation remains incomplete. Nevertheless, we are confident that it will be useful for the interpretation of our experimental data.

Computation time

The simulations presented here have been carried out with COMSOL Multiphysics 5.3a run on a workstation with a Xeon E5-1620v4 processor (3.5 GHz) and 16 GB RAM under Windows 7 (64 bit). The computation time to find a set of 24 eigen-frequencies of the complete geometry was around 50 seconds.

Acknowledgements

The author would like to thank Dra. Sonia Martínez Hedo (SGAI-CSIC) for technical support with COMSOL Multiphysics.

References

1. H. Daido, M. Nishiuchi, and A.S. Pirozhkov, Review of laser-driven ion sources and their applications, *Rep. Prog. Phys.* **75**, 056401 (2012)
2. F.S. Felber, Dipole radio-frequency power from laser plasmas with no dipole moment, *Appl. Phys. Lett.* **86**, 231501 (2005)
3. Z.-Y. Chen, J.-F. Li, J. Li, and Q.-X. Peng, Microwave radiation mechanism in a pulse-laser-irradiated Cu foil target revisited, *Physica Scripta* **83**, 055503 (2011)
4. J. Cikhardt *et al.*, Measurement of the target current by inductive probe during laser interaction on terawatt laser system PALS, *Rev. Sci. Instrum.* **85**, 103507 (2014)
5. M.J. Mead *et al.*, Electromagnetic pulse generation within a petawatt laser target chamber, *Rev. Sci. Instrum.* **75**, 4225 (2004)
6. J.E. Bateman and M.J. Mead, Electro-magnetic pulse generation in petawatt laser shots, Tech. Rep. RAL-TR-2012-005, STFC Rutherford Appleton Laboratory, 2012
7. P. Bellido *et al.*, Characterization of protons accelerated from a 3 TW table-top laser system, *J. Inst.* **12**, T05001 (2017)
8. M. De Marco *et al.*, Measurement of electromagnetic pulses generated during interactions of high power lasers with solid targets, *J. Inst.* **11**, C06004 (2016)
9. S. Ramo, J. Whinnery, and T. van Duzer, *Fields and Waves in Communication Electronics*, 3rd edition, pp. 496-499. John Wiley and Sons (1965, 1993)
10. C.A. Balanis, *Advanced Engineering Electromagnetics*, 2nd edition, pp. 483-508. John Wiley and Sons (1989, 2012)
11. COMSOL Multiphysics Application gallery, "Computing Q-factors and resonant frequencies of cavity resonators", Application ID 9618, https://www.comsol.es/model/computing-q-factors-and-resonant-frequencies-of-cavity-resonators-9618

12. COMSOL Multiphysics Application gallery, “Dipole antenna”, Application ID 8715, https://www.comsol.es/model/dipole-antenna-8715
13. J. Krása *et al.*, Spectral and temporal characteristics of target current and electromagnetic pulse induced by nanosecond laser ablation, *Plasma Phys. Control. Fusion* **59**, 065007 (2018)
14. F. Consoli *et al.*, EMP characterization at PALS on solid-target experiments, *Plasma Phys. Control. Fusion* **60**, 105006 (2018)